GBE

Genome Biology and Evolution

SMBE

Whole-Genome Comparative Analysis of Two Carbapenem-Resistant ST-258 *Klebsiella pneumoniae* Strains Isolated during a North-Eastern Ohio Outbreak: Differences within the High Heterogeneity Zones

María Soledad Ramirez[1], Gang Xie[2], German M. Traglia[3], Shannon L. Johnson[2], Karen W. Davenport[2], David van Duin[4], Azam Ramazani[1,5], Federico Perez[6], Michael R. Jacobs[7], David J. Sherratt[5], Robert A. Bonomo[6,7], Patrick S.G. Chain[3] and Marcelo E. Tolmasky[1,*]

[1]Center for Applied Biotechnology Studies, Department of Biological Science, California State University Fullerton, Fullerton, CA

[2]Bioscience Division Los Alamos National Laboratory, Los Alamos, NM

[3]IMPaM (UBA-CONICET), University of Buenos Aires, Buenos Aires, Argentina

[4]Division of Infectious Diseases, University of North Carolina, Chapel Hill, NC

[5]Department of Biochemistry, University of Oxford, United Kingdom

[6]Louis Stokes Cleveland Department of Veterans Affairs Medical Center, Cleveland, OH

[7]Department of Medicine, Case Western Reserve University School of Medicine, Cleveland, OH

*Corresponding author: E-mail: mtolmasky@fullerton.edu.

Accepted: May 31, 2016

Data deposition: These projects have been deposited at DDBJ/ENA/Genbank under the accession numbers AQRD01000000 and AQPG01000000.

Abstract

Klebsiella pneumoniae has become one of the most dangerous causative agents of hospital infections due to the acquisition of resistance to carbapenems, one of the last resort families of antibiotics. Resistance is usually mediated by carbapenemases coded for by different classes of genes. A prolonged outbreak of carbapenem-resistant *K. pneumoniae* infections has been recently described in northeastern Ohio. Most strains isolated from patients during this outbreak belong to MLST sequence type 258 (ST258). To understand more about this outbreak two isolates (strains 140 and 677), one of them responsible for a fatal infection, were selected for genome comparison analyses. Whole genome map and sequence comparisons demonstrated that both strains are highly related showing 99% average nucleotide identity. However, the genomes differ at the so-called high heterogeneity zone (HHZ) and other minor regions. This study identifies the potential value of the HHZ as a potential marker for *K. pneumoniae* clinical and epidemiological studies.

Key words: whole genome mapping, optical map, ST-258, carbapenem, KPC.

Introduction

Klebsiella pneumoniae is the causative agent of numerous infectious diseases (Woloj, et al. 1986; Daza et al. 2001; Liam, et al. 2001; Huang, et al. 2013; Suzuki et al. 2013; Ramirez et al. 2014a, b; Alcantar-Curiel and Giron 2015; Lin et al. 2015; Qu et al. 2015; Zowawi et al. 2015) and can also act as triggering factor in the initiation and development of ankylosing spondylitis and Crohn's disease (Ebringer et al. 2007; Rashid and Ebringer 2007; Rashid et al. 2013). *K. pneumoniae* strains recently acquired genes coding for carbapenemases (Nordmann et al. 2009; Munoz-Price et al. 2013; Xie et al. 2013; Ramirez, et al. 2014b), which increased the severity of the infections by complicating treatments (Hirsch and Tam 2010; van Duin et al. 2014). As a consequence, numerous groups studied aspects of virulence, antibiotic resistance, and epidemiology of carbapenem-resistant *K. pneumoniae*

© The Author 2016. Published by Oxford University Press on behalf of the Society for Molecular Biology and Evolution.
This is an Open Access article distributed under the terms of the Creative Commons Attribution Non-Commercial License (http://creativecommons.org/licenses/by-nc/4.0/), which permits non-commercial re-use, distribution, and reproduction in any medium, provided the original work is properly cited. For commercial re-use, please contact journals.permissions@oup.com

Downloaded from http://gbe.oxfordjournals.org/ at Sistema de Bibliotecas y de Información Universidad de Buenos Aires on August 4, 2016

Genome Biology and Evolution SMBE

(CR*Kp*) infections (Lin et al. 2008; Endimiani et al. 2009; Shu, et al. 2009; Hirsch and Tam 2010; Ramirez et al. 2012; Deleo et al. 2014). In one study, a combination of whole genome mapping (WGM) and whole genome sequencing (WGS) led to the identification of a particular chromosome segment, known as high heterogeneity zone (HHZ), later also called region of divergence (rd). The HHZ shows high variability and includes a "hot spot", also known as *attO* hot spot, where DNA fragments of a different origin can be inserted, and the capsular polysaccharide biosynthesis gene cluster (CPC) (Lin et al. 2008; Shu et al. 2009; Ramirez et al. 2012; Deleo et al. 2014).

An outbreak of CR*Kp* infection recently occurred in northeastern Ohio with most strains belonging to MLST sequence type 258 (ST258) (van Duin et al. 2014). To characterize KPC-producing strains causing this outbreak we analyzed two isolates that led to different outcomes after treatment. Our results showed high homogeneity at the genomic level, but significant differences occurred at one region within the HHZ.

Results and Discussion

Cases Description

Klebsiella pneumoniae Kb140 is a blood isolate from a 64-year-old man with a history of coronary artery disease, congestive heart failure, peptic ulcer disease, and chronic obstructive pulmonary disease (which was treated with chronic corticosteroids) that was transferred from an outside facility to a referral hospital to be treated for pneumonia (Ramirez et al. 2014b). Despite antibiotic treatment (intravenous tigecycline) and other procedures the patient died on hospital day 8. *K. pneumoniae* Kb677 was isolated from of urine culture of an 87-year-old woman with a history of localized breast cancer without metastases who was admitted to a referral hospital from the community (Ramirez et al. 2014b). She did not meet CDC/NHSN criteria for urinary tract infection, and was not treated with any antibiotics with *in vitro* activity against CR*Kp*. She was discharged back to her home after a prolonged hospital stay of 28 days. The antimicrobial susceptibilities of both isolates are summarized in table 1. Significant differences are that Kb140 is susceptible to gentamicin, but not to tobramycin or amikacin; and Kb677 is susceptible to amikacin but not gentamicin or tobramycin.

Table 1

Antimicrobial Susceptibility of *K. pneumoniae* Isolates Kb140 and Kb677

Antibiotic	Kb140		Kb677	
	MIC (μg/mL)	Interpretation	MIC (μg/mL)	Interpretation
Amikacin	32	I	≤4	S
Aztreonam	>16	R	>16	R
Ciprofloxacin	>2	R	>2	R
Colistin	0.5	S	0.5	S
Doripenem[a]	>2	R	2	I
Doxycycline	16	R	>16	R
Ertapenem	>4	R	>4	R
Cefepime	>16	R	8	I
Cefotaxime	>32	R	32	R
Ceftazidime	>16	R	>16	R
Gentamicin	≤1	S	>8	R
Imipenem	>8	R	8	R
Levofloxacin	>8	R	>8	R
Meropenem	>8	R	8	R
Minocycline	16	R	>16	R
Piperacillin/tazobactam	>64/128	R	>64/128	R
Polymyxin B	0.5	S	0.5	S
Trimethoprim/sulfamethoxazole	>4/76	R	>4/76	R
Tigecycline[a]	2	S	4	I
Tobramycin	>8	R	>8	R

[a]Values for doripenem and tigecycline are too close (one dilution) to assure that their phenotypes are actually different.

Whole Genome Map Comparison

The HHZ can be divided into distinct regions of which 3 and 4 seem to exhibit the highest variability (Ramirez et al. 2012). Region 3 consists of a "hot spot", also known as *attO* (Lin et al. 2008), for insertion of DNA fragments. In at least one strain, NTUH-K2044, the insertion in Region 3 is the ICE*Kp1*, a ca. 76-kbp integrative and conjugative element that includes a high-pathogenicity island (Lin et al. 2008). HHZ Region 4 contains the CPC (Ramirez et al. 2012), which shows high variability among strains (Shu et al. 2009). Comparison of WGMs of strains Kb140 and Kb677 revealed that, although not identical, their genomes are very similar (regions in blue, fig. 1*a*). One of the areas of difference (white in the WGMs) is located within the HHZ (fig. 1*a* and *b*), more precisely, at Region 4 (fig. 1*b*). Further WGM comparisons showed that both strains are closely related to *K. pneumoniae* VA360, a strain isolated in the same region before the beginning of the surveillance study, strain Kb140 being the most similar (fig. 1*c*) (Ramirez et al. 2012; Xie et al. 2013).

WGS: Comparison of the HHZs

The genomes of strains Kb140 and Kb677 are 5,677,714 and 5,894,762-bp long, respectively. Analysis of the HHZs at the nucleotide level showed that the Region 3 of both strains, as well as that of strain VA360, includes the same DNA fragment, an indication of relatedness. A comparison of the Region 3 of all three strains and those of well-studied strains such as NTUH-K2044, KCTC2242, which include unique DNA fragments, and MGH 78578, which does not include an insert is shown in figure 2*a*.

Region 3 of strains Kb140, Kb677, and VA360 includes elements coding for functions involved in conjugation, a

Downloaded from http://gbe.oxfordjournals.org/ at Sistema de Bibliotecas y de Información Universidad de Buenos Aires on August 4, 2016

Genome Biology and Evolution

SMBE

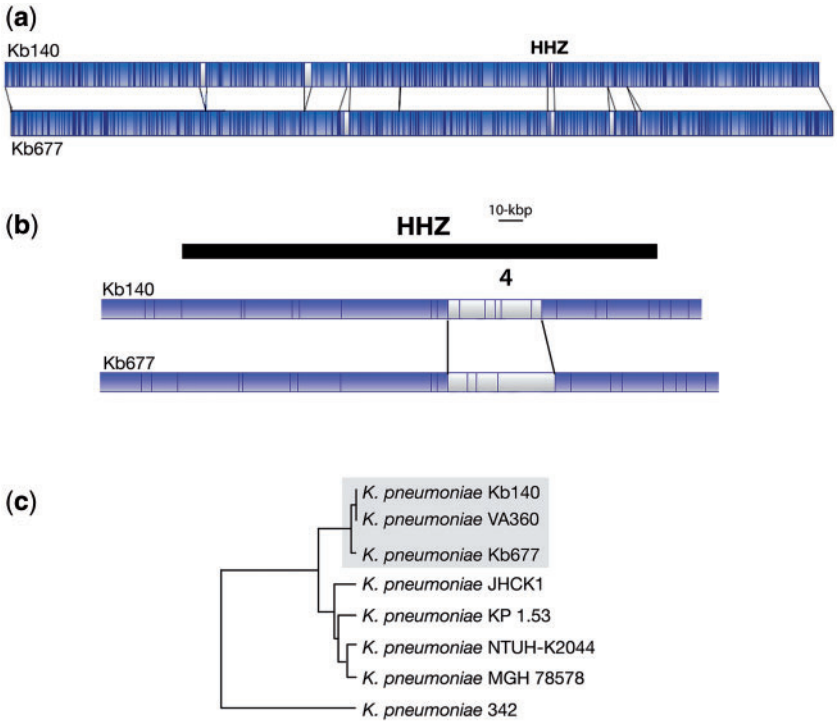

Fig. 1.—Genomic comparisons. (*a*) The *K. pneumoniae* Kb140 and Kb677 whole genome maps were compared using the MapSolver 3.2.0 software. The blue and white regions represent matching and nonmatching DNA fragments, respectively. The location of the HHZ is indicated. (*b*) Zoom-in the HHZ region. (*c*) Map similarity cluster showing *K. pneumoniae* Kb140 and Kb677 in relation to other completely sequenced *K. pneumoniae* strains. Dendogram was generated using Unweighted Pair Group Method with Arithmetic Mean. The strains Kb140, Kb670, and the closely related VA360 are boxed.

type III restriction endonuclease and the cognate methylase as well as a P4-like integrase and other hypothetical genes with unknown function (table 2). The integrase is found in numerous genomes of Gram-negatives (supplementary fig. 1S, Supplementary Material online) and its amino acid sequence shares 50% identity and 68% similarity with the ICE*Kp*1 integrase (Lin et al. 2008) (supplementary fig. S2, Supplementary Material online). As it is the case in ICE*Kp*1, the integrase could mediate insertion and excision of this DNA fragment. The Region 3 of strains Kb140, Kb677, and VA360 was also found in sixteen CR*Kp* strains (supplementary fig. S3*a*, Supplementary Material online) (Snitkin et al. 2012).

A comparison of the HHZ Region 4 among strains Kb140, Kb677, and VA360 showed that while the CPCs were identical in strains Kb140 and VA360, they were significantly different from that of strain Kb677 (fig. 2*b*). BLAST analyses of both versions of Region 4 indicated that only ten completed genomes include a CPC identical to that of strain Kb140 (supplementary fig. S3*b*, Supplementary Material online). Conversely, the CPC from strain Kb677 was found in 11 strains, 3 of them the KPNIH10, 30660/NJST258_1, and 30684/NJST258_2 that also have identical versions of HHZ Region 3 (supplementary fig. S3*c*, Supplementary Material online). There is a conspicuous GC% difference in value at the HHZ with respect to the rest of the genome at the locations corresponding to the Regions 3 and 4 (see fig. 3).

WGS: Multiple Genome Alignment and Genomic Features

The nucleotide sequences of both strains showed 99% average identity. MAUVE alignment including the *K. pneumoniae* VA360, NTUH-K2044, and MGH 78578 genomes identified seven locally collinear blocks (LCBs) and no inversions (fig. 4). A 5,757-nucleotides deletion was observed in the Kb677 genome. The deleted fragment includes genes coding for homologs to a two-component regulatory system, a heat shock protein, a putative LuxR regulator, the competence damage-inducible protein A, and a hypothetical protein. A 2,096-nucleotide deletion coding for the 23S ribosomal RNA was identified in the Kb140 genome. Furthermore, 5 and 14 unique regions were found in the Kb140 and Kb677 genomes, respectively. Three of them are prophage-like sequences and considerably larger than the rest (table 3 and fig. 3).

In both genomes 73% of the genes were assigned to a functional category including carbohydrate and amino acid metabolism, transcription and energy production and conversion (table 4). As expected, there was no significant difference in functional categories between the five strains (table 4).

Downloaded from http://gbe.oxfordjournals.org/ at Sistema de Bibliotecas y de Información Universidad de Buenos Aires on August 4, 2016

Genome Biology and Evolution SMBE

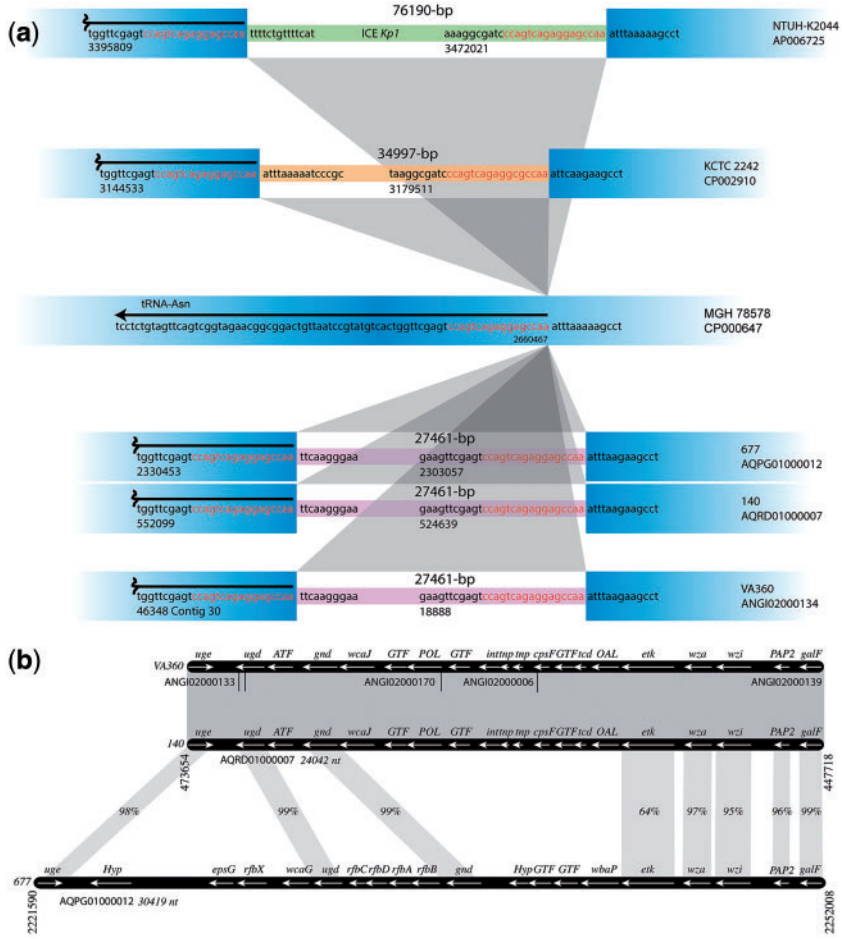

Fig. 2.—HHZ Regions 3 and 4. (*a*) Schematic diagram of the Region 3 within the HHZs of several *K. pneumoniae* strains. The DNA sequences surrounding the hot spot and inserted fragments are represented in blue. The inserted regions are shown in thinner lines with different colors to indicate that the sequences are different. The sequences inserted in strains Kb140, Kb677, and VA360 are identical. The coordinates are those found in GenBank. The hot spot sequences, also known as *attO* (Lin et al. 2008), are red and the sequences immediately adjacent to the hot spots are black. In the case of strain NTUH-K2044 the inserted sequenced is the ICE*Kp1* pathogenicity island. (*b*) Schematic comparison of the Region 4, which consists of the CPC, within the HHZs of *K. pneumoniae* strains Kb140, Kb677, and VA360. Grayed regions represent high homology. In those cases where there is no 100% identity, the identity percentage is shown. In the case of strain VA360, the Region 4 was put together using different contigs, which are identified by their accession numbers. Coordinate numbers are those in GenBank. Potential function of genes (Kelly and Whitfield 1996; Whitfield 2006; Shu et al. 2009): *uge*, UDP-galacturonate 4-epimerase; *ugd*, UDP-glucose dehydrogenase; ATF, acyl transferase; *gnd*, gluconate-6-phosphate dehydrogenase; *wcaJ*, undecaprenyl-phosphate glycosyltransferase; GTF, glycosyl transferase; POL, polysaccharide biosynthesis; *int*, integrase-like; *tnp*, transposase-like; *cpsF*, CMP-N-acetylneuraminic acid synthetase; tcd, glycosyltransferase; OAL, O-antigen ligase; *etk*, tyrosine-protein kinase; *wza*, polysaccharide export lipoprotein; *wzi*, integral outer membrane protein; PAP2, PAP2 superfamily; *galF*, modulator of GalU to elevate the cellular concentration of UDP-glucose; Hyp, hypothetical; *epsG*, putative capsular polysaccharide biosynthesis protein; *rfbX* (*wzx*), flippase; *wcaG*, GDP-4-keto-6-deoxy-D-mannose 3,5-epimerase/reductase; *rfbAB*, ATP-binding cassette transporter; *rfbC*, involved in polysaccharide synthesis (epimerase), *rfbD*, involved in polysaccharide transport; *wbaP*, membrane protein that helps transfer a galactose residue from UDP-Gal to undecaprenol diphosphate to form Gal-p-UndP.

Conclusions

The importance of *K. pneumoniae* as a pathogen has significantly grown in recent years (Nordmann et al. 2009). This is, at least in part, due the rise of strains that are becoming resistant to most antibiotics used in standard treatments. In particular, the relatively recent acquisition of carbapenemase genes led to dissemination of CR*Kp* strains that are the hardest to treat (Nordmann, et al. 2009; Munoz-Price et al. 2013; Xie et al. 2013; Ramirez et al. 2014b). These facts led us and other research groups to carry out comparative genomics studies that may help understanding the epidemiology and dissemination of CR*Kp* strains.

Here, we compared the genomes of two strains isolated during an outbreak of CR*Kp* infection in northeastern Ohio.

Downloaded from http://gbe.oxfordjournals.org/ at Sistema de Bibliotecas y de Información Universidad de Buenos Aires on August 4, 2016

Genome Biology and Evolution

SMBE

Table 2

Summary of main ORFs found in Region 3

Putative function	Coordinates		
	Kb140 AQRD01000007	Kb677 AQPG01000012	VA360 ANGI02000134
Hypothetical protein—DNA-binding family protein	c (528973.529680)	c (2307327.2308034)	c (23222.23929)
tRNA_anti-like family protein	531400.531966	2309754.2310320	25649.26215
Putative DNA-directed RNA polymerase	531981.532532	2310335.2310886	26230.26781
TIR domain protein	c (532862.533281)	c (2311216.2311635)	c (27111.27530)
Tetratricopeptide repeat family protein	c (533283.534548)	c (2311637.2312902)	c (27532.28797)
MobA/MobL family protein	c (535635.537155)	c (2313989.2315509)	c (29884.31404)
Hypothetical protein	538002.538484	2316356.2316838	32251.32733
Conserved hypothetical protein	539844.540359	2318198.2318713	34093.34608
TraD	540459.540782	2318813.2319136	34708.35031
Type IV pilin	541350.541919	2319704.2320273	35599.36168
PilV—tail fiber protein	542123.543682	2320477.2322036	36372.37931
Type III restriction endonuclease subunit R	c (544145.547105)	c (2322499.2325459)	c (38394.41354)
DNA methyltransferase	c (547115.548965)	c (2325469.2327319)	c (41364.43214)
SpnT	549159.550547	2327513.2328901	43408.44796
Phage integrase	c (550619.551893)	c (2328973.2330247)	c (44868.45566)*

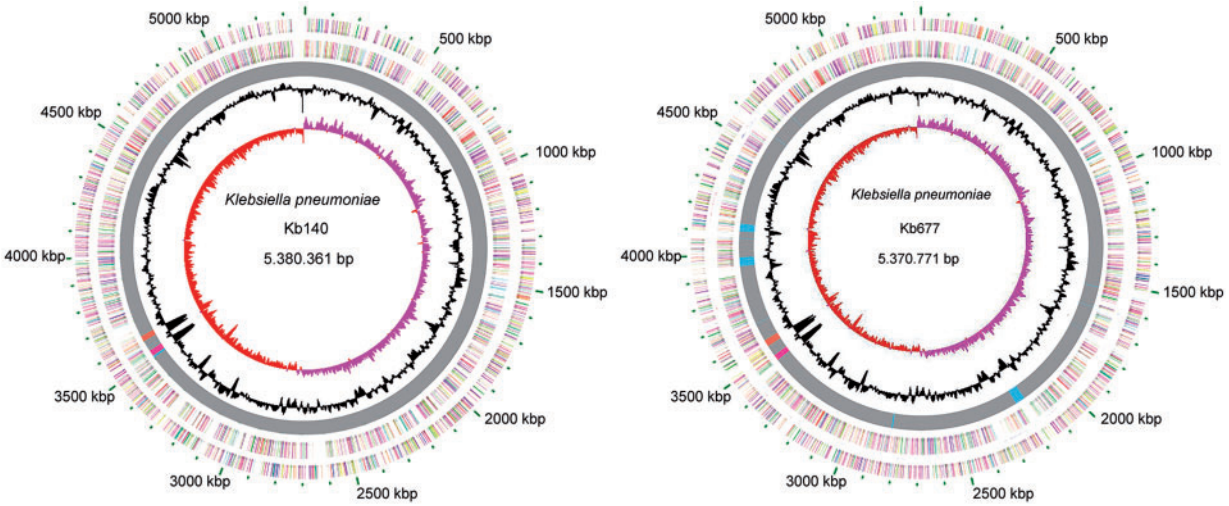

Fig. 3.—Circular genome representation of the Kb140 and Kb677 genomes. Ring 1: ORF distribution, plus strand. Ring 2: ORF distribution, negative strand. ORFs are color coded based on COG classifications. Ring 3: Common regions and unique regions are represented in gray or colors, respectively. Pink and orange correspond to HHZ Regions 3 and 4. Ring 4: GC content. Ring 5: GC skew, calculated in Artemis.

Although strains Kb677 and Kb140 differ in the carbapenemase gene they carry, only minor differences were detected between their genomes, in general due to insertions and deletions. This was not surprising because as others and we have previously observed comparing other *K. pneumoniae* strains (Deleo et al. 2014; Ramirez et al. 2014b; Sabirova et al. 2016), the genomes of this bacterium seem to be quite homogeneous. However, in spite of the similarities between both genomes, strains Kb677 and Kb140 show significant differences at the HHZ. This region, also known as "rd", was shown to be one of the most variable in *K. pneumo*niae isolates (Deleo et al. 2014). These results underscore the potential importance of the HHZ. This study shows that two strains isolated during the same outbreak could be quickly differentiated by their HHZs. We propose that this zone of the *K. pneumoniae* genome can be used as a signature for epidemiology analysis.

Downloaded from http://gbe.oxfordjournals.org/ at Sistema de Bibliotecas y de Información Universidad de Buenos Aires on August 4, 2016

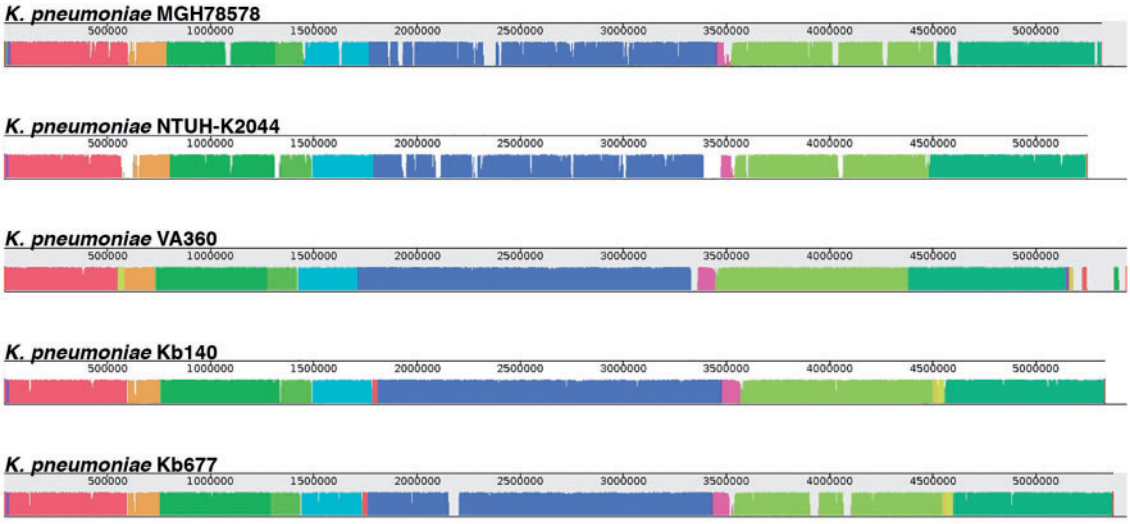

Fig. 4.—Alignment of *K. pneumoniae* strains genomes using MAUVE. Each genome's panel contains a scale showing the sequence coordinates, colored blocks that represent regions of the genome sequence that aligned to part of the other genomes, and a single black horizontal center line where the blocks that lie above are in the forward orientation (in this case there are no blocks in reverse orientation, then the lines look to be at the bottom across the genome).

Table 3
Unique Region of *K. pneumoniae* Kb140 and Kb677

Strain	Unique region	Length size (bp)	Description
Kb140	1	866	Second copy of DNA polymerase
	2	5245	Genes related to nucleotide metabolism
	3	1699	Putative regulator genes and efflux pump protein
	4	1255	Efflux pump
	5	1186	Transposase
Kb677	1	1687	Transposase and hypothetical proteins
	2	1199	Efflux pump protein
	3	800	Partial transposase sequences gene
	4	46988	Prophage insertion into the outer membrane protein W
	5	6571	Genes related to carbohydrate metabolism
	6	1366	Putative transposase
	7	41536	Phage-like proteins
	8	1961	Transposase, integrase and hypothetical protein
	9	36458	Phage-like proteins
	10	1667	Genes related to cell wall biogenesis/degradation and DNA repair
	11	1326	Putative transposase

Materials and Methods

Bacterial Strains

Klebsiella pneumoniae Kb140 and Kb677 belong to ST-258 possess a different rep-PCR type (type-A for Kb140 and type-B for Kb677). Strain Kb140 harbors bla_{KPC-2} while Kb677 harbors bla_{KPC-3}. Their antimicrobial susceptibilities were determined by broth microdilution according to CLSI methods and interpretations (Clinical-Laboratory-Standard-Institute 2012).

Genomic Analyses

The available scaffolds for the strains Kb140 and Kb677 (accession number AQRD01000000 and AQPG01000000, respectively) were ordered and oriented with the MAUVE Contig Mover (Darling et al. 2010), using the *K. pneumoniae* NTUH-K2044 genome as reference (accession number AP006725). Genomes were aligned with the open-source MAUVE aligner version 2.3.1 using the progressive algorithm. The alignments were generated using the default settings (http://darlinglab.org/mauve/mauve.html, last accessed June 8, 2016). Conserved segments that appear to be internally free from genome rearrangements, known as LCBs, were identified using MAUVE. Functional categories groups for genes have been predicted by comparison with the Clusters of Orthologous Groups (COGs) (Tatusov et al 1997). The prediction of coding sequences (CDS) was made by Rast version 4.0 software and confirmed by BLAST (Aziz et al. 2008). tRNA genes were identified using tRNAscan-SE (Lowe and Eddy

Genome Biology and Evolution SMBE

Downloaded from http://gbe.oxfordjournals.org/ at Sistema de Bibliotecas y de Información Universidad de Buenos Aires on August 4, 2016

Genome Biology and Evolution

SMBE

Table 4

COGs Between *K. pneumoniae* Strains

COG function	MGH 78578	NTUH-K2044	VA360	Kb140	Kb677
Information storage and processing					
[J] Translation, ribosomal structure and biogenesis	210	203	227	224	222
[A] RNA processing and modification	1	1	1	1	1
[K] Transcription	489	481	504	493	496
[L] Replication, recombination and repair	187	196	233	238	242
[B] Chromatin structure and dynamics	1	1	1	1	1
Cellular processes and signaling					
[D] Cell cycle control, cell division, chromosome partitioning	42	41	42	40	40
[V] Defense mechanisms	64	57	64	67	65
[T] Signal transduction mechanisms	192	190	174	171	169
[M] Cell wall/membrane/envelope biogenesis	251	251	293	289	294
[N] Cell motility	69	59	53	53	51
[U] Intracellular trafficking and secretion	113	110	113	113	112
[O] Post-translational modification	151	156	192	183	183
Metabolism					
[C] Energy production and conversion	308	304	370	365	363
[G] Carbohydrate transport and metabolism	586	593	653	644	643
[E] Amino acid transport and metabolism	613	606	594	584	600
[F] Nucleotide transport and metabolism	97	100	113	112	112
[H] Coenzyme transport and metabolism	190	191	205	203	203
[I] Lipid transport and metabolism	135	132	159	157	159
[P] Inorganic ion transport and metabolism	418	418	395	423	393
[Q] Secondary metabolites biosynthesis	122	127	78	77	77
Poorly characterized					
[R] General function prediction only	680	667	674	665	667
[S] Function unknown	382	370	370	369	373

1997). Circos software was used to represent both genomes showing Open reading frame (ORF) sorted by COGs, Unique region, Region III and IV of HHZ and GC content and skew. WGMs generated at OpGen Technologies, Inc. (Gaithersburg, MD) were also used to perform the first comparison and analyzed comparing the *Afl*II restriction maps using the MapSolver software (version 3.2.0).

Supplementary Material

Supplementary figures S1–S3 are available at *Genome Biology and Evolution* online (http://www.gbe.oxfordjournals.org/).

Funding

This study was supported by Public Health Service grant 2R15AI047115-04 from the National Institute of Allergy and Infectious Diseases, National Institutes of Health (to M.E.T.), R01AI063517 and R01AI10056 (to R.A.B.), the U.S. Department of Energy Joint Genome Institute through the Office of Science of the U.S. Department of Energy under contract no. DE-AC02-05CH11231, and Wellcome Trust Program Grant WT083469 (to D.J.S.). The Cleveland Department of Veterans Affairs, the Veterans Affairs Merit Review Program award number 1I01BX001974, and the Geriatric Research Education and Clinical Center VISN 10 supported R.A.B. A.R. was supported by the LA Basin Minority Health and Health Disparities International Research Training Program (MHIRT) 5T37MD001368.

Literature Cited

Alcantar-Curiel MD, Giron JA. 2015. *Klebsiella pneumoniae* and the pyogenic liver abscess: implications and association of the presence of *rpmA* genes and expression of hypermucoviscosity. Virulence 6:407–409.

Aziz RK, et al. 2008. The RAST Server: rapid annotations using subsystems technology. BMC Genomics 9:75.

Clinical-Laboratory-Standard-Institute. 2012. Methods for Dilution Antimicrobial Susceptibility Tests for Bacteria That Grow Aerobically; Approved standard - Ninth edition. M07–A09.

Darling AE, Mau B, Perna NT. 2010. progressiveMauve: multiple genome alignment with gene gain, loss and rearrangement. PLoS One. 5: e11147.

Deleo FR, et al. 2014. Molecular dissection of the evolution of carbapenem-resistant multilocus sequence type 258 *Klebsiella pneumoniae*. Proc Natl Acad Sci U S A. 111:4988–4993.

Daza R, Gutierrez J, Piedrola G. 2001. Antibiotic susceptibility of bacterial strains isolated from patients with community-acquired urinary tract infections. Int J Antimicrob Agents 18:211–215.

Ebringer A, Rashid T, Tiwana H, Wilson C. 2007. A possible link between Crohn's disease and ankylosing spondylitis via *Klebsiella* infections. Clin Rheumatol. 26:289–297.

Endimiani A, et al. 2009. Characterization of blaKPC-containing *Klebsiella pneumoniae* isolates detected in different institutions in the Eastern USA. J Antimicrob Chemother. 63:427–437.

Downloaded from http://gbe.oxfordjournals.org/ at Sistema de Bibliotecas y de Información Universidad de Buenos Aires on August 4, 2016

Hirsch EB, Tam VH. 2010. Detection and treatment options for *Klebsiella pneumoniae* carbapenemases (KPCs): an emerging cause of multidrug-resistant infection. J Antimicrob Chemother. 65:1119–1125.
Huang HY, Wu YH, Kuo CF. 2013. *Klebsiella pneumoniae* sepsis with unusual cutaneous presentation of generalized pustulosis. Clin Exp Dermatol. 38:626–629.
Kelly RF, Whitfield C. 1996. Clonally diverse *rfb* gene clusters are involved in expression of a family of related D-galactan O antigens in *Klebsiella* species. J Bacteriol. 178:5205–5214.
Liam CK, Lim KH, Wong CM. 2001. Community-acquired pneumonia in patients requiring hospitalization. Respirology 6:259–264.
Lin TL, Lee CZ, Hsieh PF, Tsai SF, Wang JT. 2008. Characterization of integrative and conjugative element ICE*Kp1*-associated genomic heterogeneity in a *Klebsiella pneumoniae* strain isolated from a primary liver abscess. J Bacteriol. 190:515–526.
Lin YT, Pan YJ, Lin TL, Fung CP, Wang JT. 2015. Transfer of CMY-2 ephalosporinase from *Escherichia coli* to virulent *Klebsiella pneumoniae* causing a recurrent liver abscess. Antimicrob Agents Chemother. 59:5000–5002.
Lowe TM, Eddy SR. 1997. Nucleic Acids Res. 25:955–964.
Munoz-Price LS, et al. 2013. Clinical epidemiology of the global expansion of *Klebsiella pneumoniae* carbapenemases. Lancet Infect Dis. 13:785–796.
Nordmann P, Cuzon G, Naas T. 2009. The real threat of *Klebsiella pneumoniae* carbapenemase-producing bacteria. Lancet Infect Dis. 9:228–236.
Qu TT, et al. 2015. Clinical and microbiological characteristics of *Klebsiella pneumoniae* liver abscess in East China. BMC Infect Dis. 15:161.
Ramirez MS, Traglia GM, Lin DL, Tran T, Tolmasky ME. 2014a. Plasmid-mediated antibiotic resistance and virulence in gram-negatives: the Klebsiella pneumoniae paradigm. Microbiol Spectr. 2: PLAS-0016-2013.
Ramirez MS, et al. 2014b. Genome sequences of two carbapenemase-resistant *Klebsiella pneumoniae* ST258 isolates. Genome Announc. 2:e00558–e00514.
Ramirez MS, et al. 2012. Multidrug-resistant (MDR) *Klebsiella pneumoniae* clinical isolates: a zone of high heterogeneity (HHZ) as a tool for epidemiological studies. Clin Microbiol Infect. 18:E254–E258.
Rashid T, Ebringer A. 2007. Ankylosing spondylitis is linked to *Klebsiella*—the evidence. Clin Rheumatol. 26:858–864.
Rashid T, Wilson C, Ebringer A. 2013. The link between ankylosing spondylitis, Crohn's disease, *Klebsiella*, and starch consumption. Clin Dev Immunol. 2013:872632.
Sabirova JS, Xavier BB, Coppens J, Zarkotou O, Lammens C, Janssens L, Burggrave R, Wagner T, Goossens H, Malhotra-Kumar S. 2016. Whole-genome typing and characterization of *bla*VIM19-harbouring ST383 *Klebsiella pneumoniae* by PFGE, whole-genome mapping and WGS. J Antimicrob Chemother. 71:1501–1509.
Shu HY, et al. 2009. Genetic diversity of capsular polysaccharide biosynthesis in *Klebsiella pneumoniae* clinical isolates. Microbiology 155:4170–4183.
Snitkin ES, et al. 2012. Tracking a hospital outbreak of carbapenem-resistant *Klebsiella pneumoniae* with whole-genome sequencing. Sci Transl Med. 4:148ra116.
Suzuki K, et al. 2013. Septic arthritis subsequent to urosepsis caused by hypermucoviscous *Klebsiella pneumoniae*. Intern Med. 52:1641–1645.
Tatusov RL, Koonin EV, Lipman DJ. 1997. Science. 278:631–637.
van Duin D, et al. 2014. Surveillance of carbapenem-resistant *Klebsiella pneumoniae*: tracking molecular epidemiology and outcomes through a regional network. Antimicrob Agents Chemother. 58:4035–4041.
Whitfield C. 2006. Biosynthesis and assembly of capsular polysaccharides in *Escherichia coli*. Annu Rev Biochem. 75:39–68.
Woloj M, Tolmasky ME, Roberts MC, Crosa JH. 1986. Plasmid-encoded amikacin resistance in multiresistant strains of *Klebsiella pneumoniae* isolated from neonates with meningitis. Antimicrob Agents Chemother. 29:315–319.
Xie G, et al. 2013. Genome sequences of two *Klebsiella pneumoniae* isolates from different geographical regions, Argentina (Strain JHCK1) and the United States (Strain VA360). Genome Announc. 1:e00168–e00113.
Zowawi HM, et al. 2015. The emerging threat of multidrug-resistant Gram-negative bacteria in urology. Nat Rev Urol. 12:570–584.

Associate editor: Howard Ochman

Downloaded from http://gbe.oxfordjournals.org/ at Sistema de Bibliotecas y de Información Universidad de Buenos Aires on August 4, 2016

Genome Biology and Evolution SMBE